



Enthalpy relaxation phenomena of epoxy adhesive in operational configuration: Thermal, mechanical and dielectric analyses

Nicolas Causse, Eric Dantras, Claire Tonon, Mathieu Chevalier, Hélène Combes, Pascale Guigue, Colette Lacabanne

► To cite this version:

Nicolas Causse, Eric Dantras, Claire Tonon, Mathieu Chevalier, Hélène Combes, et al.. Enthalpy relaxation phenomena of epoxy adhesive in operational configuration: Thermal, mechanical and dielectric analyses. *Journal of Non-Crystalline Solids*, 2014, vol. 387, pp. 57-61. 10.1016/j.jnoncrysol.2013.12.028 . hal-00950219

HAL Id: hal-00950219

<https://hal.science/hal-00950219>

Submitted on 21 Feb 2014

HAL is a multi-disciplinary open access archive for the deposit and dissemination of scientific research documents, whether they are published or not. The documents may come from teaching and research institutions in France or abroad, or from public or private research centers.

L'archive ouverte pluridisciplinaire **HAL**, est destinée au dépôt et à la diffusion de documents scientifiques de niveau recherche, publiés ou non, émanant des établissements d'enseignement et de recherche français ou étrangers, des laboratoires publics ou privés.



Open Archive Toulouse Archive Ouverte (OATAO)

OATAO is an open access repository that collects the work of Toulouse researchers and makes it freely available over the web where possible.

This is an author-deposited version published in: <http://oatao.univ-toulouse.fr/>
Eprints ID: 11008

Identification number: DOI : 10.1016/j.jnoncrysol.2013.12.028

Official URL: <http://dx.doi.org/10.1016/j.jnoncrysol.2013.12.028>

To cite this version:

Causse, Nicolas and Dantras, Eric and Tonon, Claire and Chevalier, Mathieu and Combes, Hélène and Guigue, Pascale and Lacabanne, Colette *Enthalpy relaxation phenomena of epoxy adhesive in operational configuration: Thermal, mechanical and dielectric analyses.* (2014) Journal of Non-Crystalline Solids, vol. 387 . pp. 57-61. ISSN 0022-3093

Any correspondence concerning this service should be sent to the repository administrator:
staff-oatao@inp-toulouse.fr

Nicolas Causse ^a, Eric Dantras ^{a,*}, Claire Tonon ^b, Mathieu Chevalier ^b, H  l  ne Combes ^c,
Pascale Guigue ^c, Colette Lacabanne ^a

^c Centre National d'Etudes Spatiales (CNES), 18 Avenue Edouard Belin, Toulouse 31401, France

Thermal cycling in space environment can cause physical aging of polymers used in structural adhesive bonded joint. Later, they can initiate failure. A methodology to follow physical aging effects on their thermal, mechanical and dielectric properties is applied to a commercial epoxy adhesive. The analytic description, using Tool, Narayanaswamy and Moynihan model gives a good description of the enthalpy relaxation. It is completed by a phenomenological analysis of the evolution of the adhesive thermal transitions, mechanical properties and molecular mobility. Tested samples with bonded assembly are representative of in service configurations. The influence of physical aging on the adhesive and the associated bonded assemblies is analyzed.

Mechanical and dielectric relaxations

Physical aging [8–10] is associated with the instability (non-equilibrium state) of amorphous materials in the glassy state. Molecular segmental rearrangements lead to a change in the molecular mobility and the free volume of the polymer to reach the

The aim of this work is to investigate physical aging phenomena on a complex commercial adhesive to verify the reliability of components and structures. Since the glass transition temperature of this adhesive is rather low, a possible long term deformation of the adhesive if subjected to a mechanical stress can occur in its operational temperature range. This study might allow us to propose a methodology providing

E-mail address: eric.dantras@univ-tlse3.fr (E. Dantras).

a complete description of physical aging phenomena of a structural bonded joint.

2. Experimental

2.1. Adhesive

The adhesive is a commercial amine–epoxy bicomposant adhesive. The two parts are prepared and a nozzle allows us to make and extrude the mix with an accurate repeatability. The precise composition is not given by the furnisher but some data are available. The hardener (part A) is a mix of several components where aliphatic amine is preponderant. The part B is based on diglycidyl ether of bisphenol-A epoxy resin mixed with other components (fillers, catalyst...). This adhesive is toughened by a blend of polybutadiene and thermoplastic copolymers. Parts A and B are mixed at room temperature (ratio 2:1). The curing process is 7 days at 21 ± 2 °C.

All the samples were heated up to 150 °C prior to the experiments to erase previous thermal history, and to stabilize the adhesive structure.

2.2. Differential scanning calorimetry

Differential scanning calorimetry (DSC) was performed on a PerkinElmer Pyris Diamond apparatus under helium. The heat flow between a reference and the sample was measured by power compensation. Uncured adhesive was cast in sealed aluminum pans. The curing process occurred in these pans: this protocol guarantees a good thermal contact between the sample and the pan. The sample weight was ranging from 5 to 15 mg.

2.3. Dynamic mechanical analysis

The dynamic mechanical analysis (DMA) was performed on a Rheometrics Scientific ARES of TA Instruments under nitrogen. Tests were carried out in torsion rectangular mode over the linear elasticity range (angular frequency $\omega = 1 \text{ rad} \cdot \text{s}^{-1}$; strain $\gamma = 0.01\%$). This technique allows us to access to the complex shear modulus $G^*(\omega, T)$:

$$G^*(\omega, T) = G'(\omega, T) + i G''(\omega, T) \quad (1)$$

where G' is the dynamic conservative modulus, and G'' is the dissipative modulus.

2.4. Thermally stimulated current analysis

The thermally stimulated current (TSC) analysis [21,27] was performed on a TSC II of Setaram under helium. The sample configuration is adapted to introduce a “gap” which limits the charge transport between the capacitor electrodes [28]. The uncured adhesive was applied in a thin layer (250–500 μm) to the aluminum circular lower electrode (diameter = 10 mm). After the curing process, two 100 μm diameter silica spacer fibers were placed between the adhesive layer free surface and the upper electrode to create the air gap (Fig. 1).



Fig. 1. Sample configuration including “air gap” for TSC experiments.

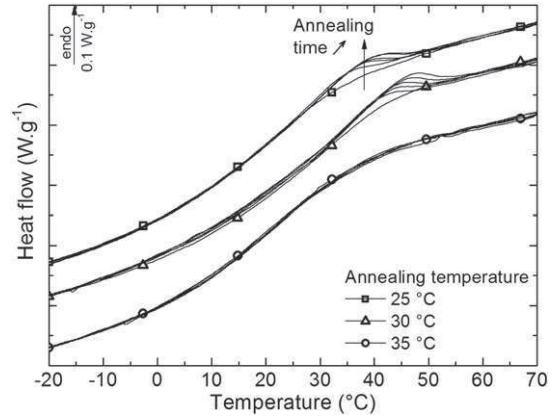


Fig. 2. DSC scans for samples after annealing for an increasing time (in the order of increasing peak intensity) at the temperature indicated against each curve.

3. Results and discussion

3.1. Enthalpy relaxation

The first thermal history [29] explored to evidence enthalpy relaxation of the adhesive is shown in Fig. 2. In the DSC apparatus, the sample is cooled from 80 °C to an annealing temperature $T_a = 25, 30$ and 35 °C just lower than T_g during an annealing time $t_a = 0, 10, 60, 120, 360$ and 600 min. The temperature is lowered to a temperature $T_0 = -50$ °C well below T_g at a rapid cooling rate (-40 °C \cdot min $^{-1}$). The thermogram is monitored during heating ($+20$ °C \cdot min $^{-1}$) to 80 °C. This protocol is useful to evaluate the effect of dwell time imposed by the normalized thermal cycling procedure. The glass transition temperature of the rejuvenated adhesive is about 25 °C.

When the annealing time is higher than 10 min, an endothermic peak is superimposed upon the sigmoidal change in the heat flow associated with the adhesive glass transition temperature. The amplitude and the maximum temperature of this peak increase with an increasing annealing time. The annealing temperature influences this overshoot: for the same annealing time the overshoot is always higher in intensity and temperature for a 30 °C annealing. The 35 °C annealing temperature is too closed to T_g to observe any effect of enthalpic relaxation: epoxy chains are in the rubbery state and are not affected. At 25 °C, the evolutions due to thermal history are slow. Differences between annealing times are limited.

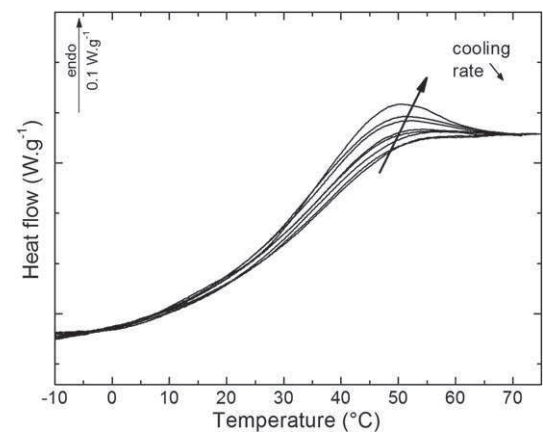


Fig. 3. DSC scans for samples after slowing cooling rates (in the order of increasing peak intensity).

In Fig. 3, the enthalpy relaxation is also analyzed as a function of the cooling rate q_c [30]. The sample is heated to 80 °C (up to its T_g). The temperature is lowered to a temperature $T_0 = -50$ °C well below T_g at a constant controlled cooling rate $q_c = -40, -20, -10, -5, -3, -1, -0.5$ and -0.25 °C · min⁻¹. The thermogram is monitored during heating ($+20$ °C · min⁻¹) to 80 °C. The thermograms show an endothermic peak superimposed on the glass transition. The peak intensity increases when the cooling rate slows down. The enthalpy relaxation is therefore greater when the cooling rate is slow. Regarding this kind of thermal history, the overshoot maximum temperature does not vary.

The peak associated to physical aging exhibits a large temperature distribution, contrary to the ones observed after annealing (Fig. 2). The glass transition temperature is largely distributed on this epoxy network due to a strong heterogeneity of the network. The “varying cooling rates” thermal history involves an enthalpic relaxation on the entire range of this distribution. The “annealing” thermal history selects only a part of the distribution:

- In the low temperature range of the transition, the annealing temperature is too far. The enthalpy relaxation kinetic is slow compared to the time scale of this kind of experiment.
- In the high temperature range, annealing occurs in the rubbery state and does not have any effect.

Both thermal histories do not influence significantly the onset and the inflection point of the transition, whatever the aging state. The Tool, Narayanaswamy and Moynihan (TNM) model [31–33] is used to describe the structural relaxation based on the fictive temperature concept, T_f , defined by Eq. (2).

$$\int_{T_f}^{T_0} (C_{p,r} - C_{p,g}) dT' = \int_T^{T_0} (C_p - C_{p,g}) dT' \quad (2)$$

where C_p is the measured heat capacity, $C_{p,g}$ and $C_{p,r}$ respectively are the heat capacities at the glassy and the rubbery states, and T_0 is the reference temperature beyond T_g wherein the system is in equilibrium.

The thermograms in Fig. 3 reflect various structural states of the network in the glassy state, dependent on the thermal history. These states are described by T_f , which is plotted in Fig. 4 as a function of temperature and cooling rate. For temperatures above the glass transition, the adhesive is in an equilibrium state (rubbery state). The fictive temperature follows the equilibrium curve $T_f = T$ for every cooling rate. In the glassy state below the glass transition, T_f departs from the equilibrium curve and reaches an asymptotic value, called the limiting fictive temperature T'_f . These values are reported in Table 1. The cooling rates of -40 °C · min⁻¹ and -20 °C · min⁻¹ result in an identical structural

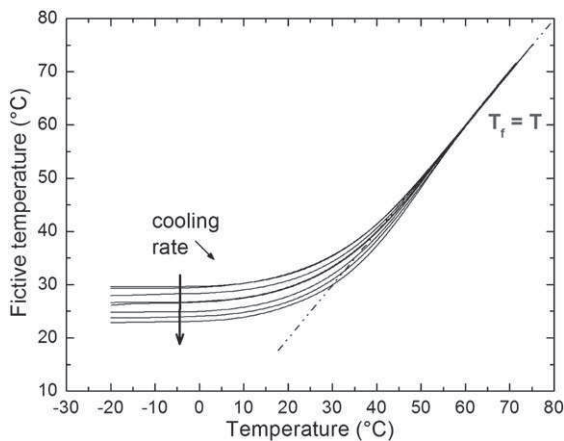


Fig. 4. Fictive temperature as a function of temperature for various cooling rates.

Table 1
Limiting fictive temperature as a function of cooling rate.

$ q_c $ (°C · min ⁻¹)	40	20	10	5	3	1	0.5	0.25
T'_f (°C)	29.6	29.4	28.3	26.7	26.6	25.0	24.0	23.0

state of the glass. For a cooling rate slower than -20 °C · min⁻¹, the limiting fictive temperature decreases when the cooling rate is slower. Error bars are associated to the determination of T_g at ± 1 °C. These values of T'_f are used to calculate the activation energy associated with the structural relaxation, thanks to Eq. (3).

$$d \ln |q_c| / d \left(1/T'_f \right) = -\Delta h^* / R \quad (3)$$

where q_c is the cooling rate, Δh^* is the activation enthalpy, and R is the gas constant.

The variation of the logarithmic value of the cooling rate is plotted as a function of the inverse of T'_f in Fig. 5. This variation is a linear function. The calculated activation energy is $\Delta h^* = 520 \pm 20$ kJ · mol⁻¹ (the uncertainty is associated with the linear regression). This value is lower than the one measured for most epoxy networks [6], however it is consistent with partially cured epoxy networks [12,34]. The adhesive studied has a longer aliphatic sequence (18 methylene groups) and it is partially cured [35]; it can explain the low value of the activation enthalpy.

3.2. Mechanical relaxations

The influence of physical aging on the adhesive mechanical properties is evaluated by dynamic mechanical analysis in Fig. 6. The protocol of varying cooling rates is extended to a larger temperature range to study the influence of cooling rate on the localized molecular mobility. The range of cooling rates available is reduced by the large temperature range studied and by sample size which limit heat transfers. The sample is heated to 150 °C. The temperature is lowered to a temperature $T_0 = -130$ °C at a constant controlled cooling rate $q_c = -5, -2, -1$ and -0.7 °C · min⁻¹. The experimental sample size and the DMA apparatus temperature control do not allow working with the same cooling rate range than with DSC. The isochronous evolution G' and G'' is recorded as a function of temperature (heating rate: 3 °C · min⁻¹).

The four thermograms recorded after each cooling rate are superimposed and do not show any significant differences. A curing study has been previously achieved and it showed that the curing is complete when the adhesive is heated up to 150 °C after the 7 day curing process at room temperature. The conservative modulus G' on the

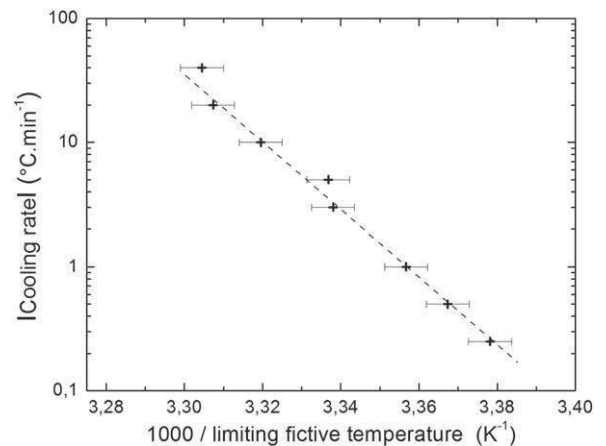


Fig. 5. Logarithm of cooling rate as a function of reciprocal T'_f .

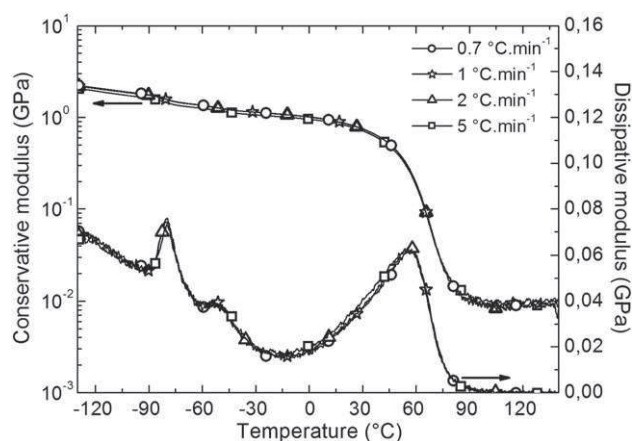


Fig. 6. Conservative and dissipative shear modulus as a function of temperature after various cooling rates.

vitreous and rubbery plateaus is equivalent whatever the thermal history.

The G'' thermograms show that the mechanical energy dissipation is equivalent in the four cases. Three relaxation modes are evidence on these thermograms [36]. The β peak at $-84 \pm 1^\circ\text{C}$ is associated with the mobility of the $\text{O}-\text{CH}_2-\text{CHOH}-\text{CH}_2$ hydroxypropylether units and/or phenyl ring flips. The α_{PBD} peak at $-54 \pm 3^\circ\text{C}$ is associated with the anelastic manifestation of the glass transition of the polybutadiene phase dispersed in the epoxy network. It is an amine terminated butadiene-acrylonitrile copolymer. The α peak at $55 \pm 1^\circ\text{C}$ is associated with the anelastic manifestation of the epoxy glass transition. The relaxation modes are not influenced by the different thermal history. Even if DSC experiments reveal that different aging states are produced by this cooling rates (Figs. 3 and 5), the analysis of the G' and G'' values does not allow their discrimination.

3.3. Dielectric relaxations

The influence of physical aging on the α -relaxation mode is investigated by thermally stimulated current (TSC) on Fig. 7. This peak is the dielectric manifestation of the glass transition. The air gap configuration makes it possible to move the conductivity front to higher temperatures and to access to α -mode signal. The presence of an interface between adhesive and metallic substrate ensures a certain representativity of the sample compared to operational configuration (adhesively bonded joint). The sample is heated to 100°C to erase its thermal history. The temperature is lowered to a temperature $T_0 = -30^\circ\text{C}$ well below T_g at a constant controlled cooling rate q_c . The sample is then

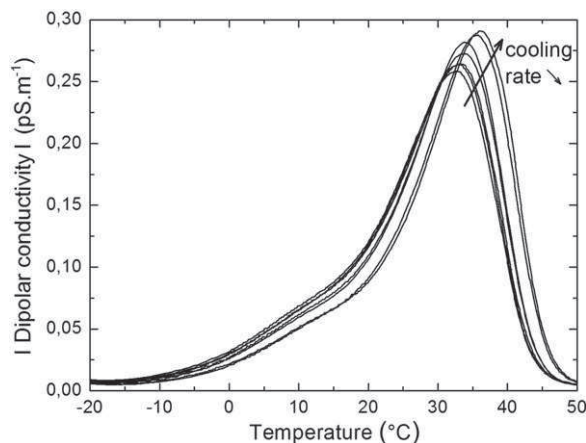


Fig. 7. Dipolar conductivity of adhesive samples after various cooling rates. A magnification at the peak maximum is shown in the insert.

subjected to an electrical field ($E = 200 \text{ V} \cdot \text{mm}^{-1}$) during heating ($+7^\circ\text{C} \cdot \text{min}^{-1}$) to 100°C . During this heating ramp, the polarization current is measured to monitor the complex relaxation spectrum.

Thermocurrents of the rejuvenated adhesive exhibit a widely distributed peak between -15°C and 50°C . Its maximum is 31°C and it has a shoulder in its low temperature range associated to network heterogeneities mobility. When the cooling rate is lowered the peak maximum temperature shifts to higher temperatures. The distribution function associated with this relaxation is also affected since the peak amplitude increases and width at half-height decreases.

Temperatures and maximum intensities of the α peak are plotted in Fig. 8 as a function of the cooling rate on a logarithmic scale. As described qualitatively in Fig. 7, the peak maximum temperature increases from 32.5°C after the cooling at $20^\circ\text{C} \cdot \text{min}^{-1}$ to 36°C after cooling at $0.25^\circ\text{C} \cdot \text{min}^{-1}$. The experimental uncertainty, due to thermal control in TCS apparatus and electrometer measurement range, induces an error of $\pm 0.5^\circ\text{C}$ and $\pm 5\text{fC} \cdot \text{m}^{-1}$. Similarly, the amplitude increases by $0.2 \text{ pS} \cdot \text{m}^{-1}$ between these two thermal histories. Changes in intensities and peak maximum temperatures are linear with the logarithm of the cooling rate. The evolution of the width at half height is not presented here: it follows a linear decrease of about 2°C between the two extreme aging states. All the evolutions of these parameters are consistent with previous studies [21,24]. They are limited, which is consistent with measurements of DSC (no change in the position of the glass transition temperature) and DMA (no change in viscoelastic properties and molecular mobility). The low frequency TSC technique is suitable to characterize slight evolutions of the molecular mobility due to physical aging.

4. Conclusion

The thermal cycling effects on the physical aging of a commercial epoxy adhesive have been studied in bonded joint configuration. A complete characterization of these phenomena is reached using static and dynamic thermal histories on thermal, mechanical and dielectric analyses. In spite of the complex formulation of the adhesive, the physical aging is well described by the TNM model in terms of enthalpy relaxation. This analytical description of physical aging shows that the aging activation energy is low. The phenomenological approach allows us to study the influence of the cooling kinetics and isothermal steps. The various thermal histories (DSC and DMA) do not influence the thermal transitions and mechanical properties of the adhesive. Since the glass transition temperature of this adhesive is rather low, a long term deformation of the adhesive if subjected to a mechanical stress remains possible in its operational temperature range. A new sample configuration has been tested to improve the relevance of dielectric measurements on adhesively bonded joints. In preserving an interface between

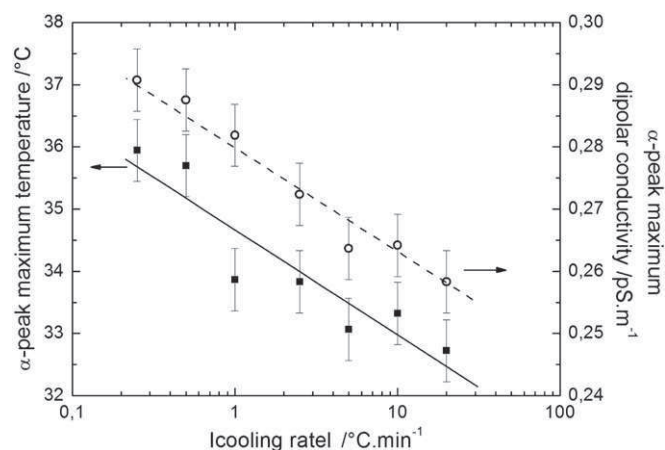


Fig. 8. Temperature and amplitude of the α -peak maximum as a function of cooling rate.

adhesive and aluminum substrate, the air gap prevents the contribution of conductivity and gives access to the dielectric manifestation of the glass transition. The efficiency of this configuration has been proved: the slight evolutions of molecular mobility at T_g can be followed. Such methodology providing thermal, mechanical and dielectric parameters associated with representative test configurations was particularly relevant to describe the physical aging of bonded assemblies.

References

- [1] E. Grossman, I. Gouzman, Space environment effects on polymers in low earth orbit, *Nucl. Inst. Methods Phys. Res. B* 208 (2003) 48–57.
- [2] European Cooperation for Space Standardization, ECSS-Q-ST-70-04C, Thermal Testing for the Evaluation of Space Materials, Processes, Mechanical Parts and Assemblies, ECSS Secretariat ESA-ESTEC Requirements & Standards Division Noordwijk, 2009.
- [3] D.B. Adolf, R.S. Chambers, B. Elisberg, M. Stavig, M. Ruff, Predicting cohesive failure in thermosets, *J. Appl. Polym. Sci.* 119 (2011) 2143–2152.
- [4] N. Causse, E. Dantras, C. Tonon, M. Chevalier, H. Combes, P. Guigue, C. Lacabanne, Environmental ageing of aerospace epoxy adhesive in bonded assembly configuration, *J. Therm. Anal. Calorim.* (2013) 1–8.
- [5] J.P. Pascault, R.J.J. Williams, Glass transition temperature versus conversion relationships for thermosetting polymers, *J. Polym. Sci. B Polym. Phys.* 28 (1990) 85–95.
- [6] G.M. Odegard, A. Bandyopadhyay, Physical aging of epoxy polymers and their composites, *J. Polym. Sci. B Polym. Phys.* 49 (2011) 1695–1716.
- [7] D.J. Plazek, Z.N. Frund, Epoxy resins (DGEBA): the curing and physical aging process, *J. Polym. Sci. B Polym. Phys.* 28 (1990) 431–448.
- [8] L.C.E. Struik, Physical aging in plastics and other glassy materials, *Polym. Eng. Sci.* 17 (1978) 165–173.
- [9] I.M. Hodge, Enthalpy relaxation and recovery in amorphous materials, *J. Non-Cryst. Solids* 169 (1994) 211–266.
- [10] J.M. Hutchinson, Physical aging of polymers, *Prog. Polym. Sci.* 20 (1995) 703–730.
- [11] S. Montserrat, Physical aging studies in epoxy resins. I. Kinetics of the enthalpy relaxation process in a fully cured epoxy resin, *J. Polym. Sci. B Polym. Phys.* 32 (1994) 509–522.
- [12] S. Montserrat, P. Cortés, Y. Calventus, J.M. Hutchinson, Effect of crosslink length on the enthalpy relaxation of fully cured epoxy-diamine resins, *J. Polym. Sci. B Polym. Phys.* 38 (2000) 456–468.
- [13] E. Dantras, J. Dandurand, C. Lacabanne, A.M. Caminade, J.P. Majoral, Enthalpy relaxation in phosphorus-containing dendrimers, *Macromolecules* 35 (2002) 2090–2094.
- [14] W.D. Cook, M. Mehrabi, G.H. Edward, Ageing and yielding in model epoxy thermosets, *Polymer* 40 (1999) 1209–1218.
- [15] L. Barral, J. Cano, J. Lopez, I. Lopez-Bueno, P. Nogueira, M.J. Abad, C. Ramirez, Physical aging of an epoxy/cycloaliphatic amine resin, *Eur. Polym. J.* 35 (1999) 403–411.
- [16] L. Barral, J. Cano, J. Lopez, I. Lopez-Bueno, P. Nogueira, M.J. Abad, C. Ramirez, Physical aging of a tetrafunctional/phenol novolac epoxy mixture cured with diamine–DSC and DMA measurements, *J. Therm. Anal. Calorim.* 60 (2000) 391–399.
- [17] S.L. Maddox, J.K. Gillham, Isothermal physical aging of a fully cured epoxy-amine thermosetting system, *J. Appl. Polym. Sci.* 64 (1997) 55–67.
- [18] A.A. Roche, J. Bouchet, S. Bentadjine, Formation of epoxy-diamine/metal interphases, *Int. J. Adhes. Adhes.* 22 (2002) 431–441.
- [19] W. Possart, J.K. Krüger, C. Wehlack, U. Müller, C. Petersen, R. Bactavatchalou, A. Meiser, Formation and structure of epoxy network interphases at the contact to native metal surfaces, *C. R. Chim.* 9 (2006) 60–79.
- [20] A. Meiser, C. Kübel, H. Schäfer, W. Possart, Electron microscopic studies on the diffusion of metal ions in epoxy-metal interphases, *Int. J. Adhes. Adhes.* 30 (2010) 170–177.
- [21] C. Lacabanne, D. Chatain, Depolarization thermocurrents in amorphous polymers, *J. Polym. Sci. Polym. Phys. Ed.* 11 (1973) 2315–2328.
- [22] S. Doulut, C. Bacharan, P. Demont, A. Bernès, C. Lacabanne, Physical aging and tacticity effects on the α relaxation mode of amorphous polymers by thermally stimulated techniques, *J. Non-Cryst. Solids* 235–237 (1998) 645–651.
- [23] C. Bacharan, C. Dessaux, A. Bernès, C. Lacabanne, Thermally stimulated current spectroscopy of amorphous and semi-crystalline polymers, *J. Therm. Anal. Calorim.* 56 (1999) 969–982.
- [24] L. Goitandia, A. Alegría, Physical aging of poly(vinyl acetate). A thermally stimulated depolarization current investigation, *J. Non-Cryst. Solids* 287 (2001) 237–241.
- [25] L. Delbreilh, M. Negahban, M. Benzohra, C. Lacabanne, J.M. Saiter, Glass transition investigated by a combined protocol using thermostimulated depolarization currents and differential scanning calorimetry, *J. Therm. Anal. Calorim.* 96 (2009) 865–871.
- [26] N. Causse, Analyse des relaxations enthalpiques, mécaniques et diélectriques pour l'étude du vieillissement d'assemblages collés structuraux, (PhD Thesis) Université Paul Sabatier, Toulouse, 2012.
- [27] G. Teyssedre, C. Lacabanne, Some considerations about the analysis of thermostimulated depolarization peaks, *J. Phys. D. Appl. Phys.* 28 (1995) 1478.
- [28] J. van Turnhout, Thermally Stimulated Discharge of Polymer Electrets: A Study on Nonisothermal Dielectric Relaxation Phenomena, Elsevier Science & Technology, 1975.
- [29] S.E.B. Petrie, Thermal behavior of annealed organic glasses, *J. Polym. Sci. A-2 Polym. Phys.* 10 (1972) 1255–1272.
- [30] J.M. Hutchinson, A.J. Kovacs, A simple phenomenological approach to the thermal behavior of glasses during uniform heating or cooling, *J. Polym. Sci. Polym. Phys. Ed.* 14 (1976) 1575–1590.
- [31] A.Q. Tool, Relation between inelastic deformability and thermal expansion of glass in its annealing range, *J. Am. Ceram. Soc.* 29 (1946) 240–253.
- [32] O.S. Narayanaswamy, A model of structural relaxation in glass, *J. Am. Ceram. Soc.* 54 (1971) 491–498.
- [33] C.T. Moynihan, A.J. Easteal, M.A. De Bolt, J. Tucker, Dependence of the fictive temperature of glass on cooling rate, *J. Am. Ceram. Soc.* 59 (1976) 12–16.
- [34] J.M. Hutchinson, D. McCarthy, S. Montserrat, P. Cortés, Enthalpy relaxation in a partially cured epoxy resin, *J. Polym. Sci. B Polym. Phys.* 34 (1996) 229–239.
- [35] M. Chevalier, Vieillessement hygrothermique d'assemblages structuraux polyepoxy: analyse de la mobilité moléculaire par spectroscopie diélectrique dynamique, (PhD Thesis) Université Paul Sabatier, Toulouse, 2008.
- [36] N. Causse, L. Quiroga Cortes, E. Dantras, C. Tonon, M. Chevalier, H. Combes, P. Guigue, C. Lacabanne, New bonded assembly configuration for dynamic mechanical analysis of adhesives, *Int. J. Adhes. Adhes.* 46 (2013) 1–6.